Acta Phys. Hung. A ?/? (?) ?–?

HEAVY ION PHYSICS

Isentropic Equation of State of Two-Flavour QCD in a Quasi-Particle Model

M. Bluhm[1], B. Kämpfer[1,2], R. Schulze[2] and D. Seipt[2]

[1] Forschungszentrum Rossendorf, PF 510119, 01314 Dresden, Germany

[2] Institut für Theoretische Physik, TU Dresden, 01062 Dresden, Germany

Received date

Abstract. We examine the isentropic QCD equation of state within a quasi-particle model being adjusted to first principle QCD calculations of two quark flavours. In particular, we compare with Taylor expansion coefficients of energy and entropy densities and with the isentropic trajectories describing the hydrodynamical expansion of a heavy-ion collision fireball.

Keywords: QCD Equation of state, Quasi-particle model
PACS: 12.38.Mh, 12.39.-x

1. Introduction

With growing evidence, ideal hydrodynamics appears to be successfully describing the expansion stage of strongly interacting matter in relativistic heavy-ion collisions [1, 2, 3, 4, 5]. The heart of hydrodynamics is the equation of state (EoS) which is needed as important interrelation among the state variables of strongly interacting matter in order to solve the hydrodynamic equations of motion. The EoS can, for instance, relate pressure, energy density and baryon density in the form $p = p(e, n_B)$. The influence of different model EoS on observables was analyzed, e. g. in [3, 6, 7]. Recent progress in QCD calculations (performed numerically on a discretized space-time grid, dubbed lattice), though, allows the calculation of these EoS quantities from first principles. It is the aim of the present paper to compare our quasi-particle model with some available lattice QCD results.

Our paper is organized as follows. In section 2 we review our quasi-particle model. In section 3, we compare the model with recent two flavour lattice QCD results for pressure, energy density and entropy density. In particular, we focus on the isentropic trajectories and the EoS along those paths of constant entropy per baryon. The results are summarized in section 4.

1219-7580/04/ $ 20.00

2. Quasi-Particle Model

The QCD EoS was often formulated in terms of quasi-particles with effectively modified properties due to the strong interaction (cf. [8, 9] and references therein). More recently developed quasi-particle models are proposed in [10, 11, 12, 13, 14, 15, 16]. In our quasi-particle model (QPM) [17], we employ as thermodynamic potential the pressure p in thermal equilibrium. Concentrating on the case of $N_f = 2$ light quark flavours with one chemical potential μ_q, p as a function of temperature T and μ_q reads

$$p(T, \mu_q) = \sum_{a=q,g} p_a - B(T, \mu_q) \tag{1}$$

with partial pressures of quarks (q) and transverse gluons (g) $p_a = d_a/(6\pi^2) \int_0^\infty dk k^4 \left(f_a^+ + f_a^-\right)/\omega_a$. Here, $d_q = 2N_f N_c$, $d_g = N_c^2 - 1$, $N_c = 3$, and $f_a^\pm = (\exp([\omega_a \mp \mu_a]/T) + S_a)^{-1}$ with $S_q = 1$ for fermions and $S_g = -1$ for bosons. Note $\mu_g = 0$.

The quasi-particles propagate predominantly on-shell with a dispersion relation approximated by the asymptotic mass shell expression near the light cone, $\omega_a = \sqrt{k^2 + m_a^2}$, where $m_a^2 = m_{0;a}^2 + \Pi_a$ [18] with self-energies Π_a and $m_{0;g} = 0$. For Π_a, we employ the asymptotic expressions of the gauge independent hard-thermal loop / hard-density loop self-energies [19]. The mean field interaction term $B(T, \mu_q)$ in (1) is determined by thermodynamic self-consistency and stationarity of the thermodynamic potential under functional variation with respect to the self-energies, $\delta p/\delta \Pi_a = 0$ [20].

Replacing the running coupling g^2 entering Π_a by an effective coupling G^2 depending on T and μ_q, non-perturbative effects within the strongly interacting system are accommodated in our model. A convenient parametrization of $G^2(T, \mu_q = 0)$ (cf. [21, 22]) is

$$G^2(T, \mu_q = 0) = \begin{cases} G^2_{2-\text{loop}}(\xi(T)), & T \geq T_c, \\ G^2_{2-\text{loop}}(\xi(T_c)) + b(1 - T/T_c), & T < T_c, \end{cases} \tag{2}$$

where $G^2_{2-\text{loop}}$ is the relevant part of the 2-loop running coupling. Here, $\xi(T) = \lambda(T - T_s)/T_c$ contains a scale parameter λ and an infrared regulator T_s. The effective coupling G^2 for arbitrary T and μ_q can be found by solving a quasi-linear partial differential equation which follows from Maxwell's relation (cf. [17, 23] for details of the model). In the next section, we want to test our phenomenological QPM by comparing with recent two-flavour ($N_f = 2$) lattice QCD results [24, 25, 26].

3. Equation of State for $N_f = 2$

For small μ_q, the pressure can be expanded into a Taylor series in powers of (μ_q/T),

$$p(T, \mu_q) = T^4 \sum_{n=0}^{\infty} c_n(T) \left(\frac{\mu_q}{T}\right)^n, \tag{3}$$

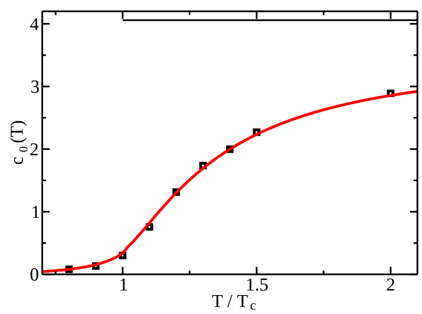

Fig. 1. Comparison of our QPM with lattice QCD results (symbols) for $c_0(T)$ as function of T/T_c for $N_f = 2$. Raw lattice QCD data [25] are continuum extrapolated by an extrapolation factor $d = 1.1$ for $T > T_c$ as advocated in [25, 27] due to finite size and cut-off effects. QPM parameters: $\lambda = 4.4$, $T_s = 0.67T_c$, $b = 344.4$, $B(T_c) = 0.31T_c^4$, setting $T_c = 175$ MeV as in [24]. The horizontal line depicts the corresponding Stefan-Boltzmann value highlighting the effects of strong interaction near T_c.

which has recently been studied in lattice QCD [25, 26]. The Taylor series was calculated up to including order $(\mu_q/T)^6$. $c_n(T)$, vanishing for odd n, follow straightforwardly from (1) through differentiation,

$$c_n(T) = \frac{1}{n!} \frac{\partial^n (p/T^4)}{\partial(\mu_q/T)^n}\bigg|_{\mu_q=0} . \qquad (4)$$

In Fig. 1, we compare QPM with lattice QCD results for $c_0(T) = p(T, \mu_q = 0)/T^4$. In analogy to the lattice simulations, we set $m_{0;q}(T) = 0.4T$. Furthermore, in [22] an impressively good agreement between the QPM results of $c_{2,4,6}(T)$ and the lattice QCD data was shown.

From (3), other thermodynamic quantities such as net baryon density $n_B = \partial p/\partial\mu_B$, entropy density s and energy density e follow as

$$s(T, \mu_B) = T^3 \sum_{n=0}^{\infty} s_n(T) \left(\frac{\mu_B}{3T}\right)^n \ , \ \ e(T, \mu_B) = T^4 \sum_{n=0}^{\infty} e_n(T) \left(\frac{\mu_B}{3T}\right)^n , \qquad (5)$$

where $e_n(T) = 3c_n(T) + c_n'(T)$ and $s_n(T) = (4-n)c_n(T) + c_n'(T)$. Here, $\mu_B = 3\mu_q$ denotes the baryo-chemical potential and $c_n'(T) = T dc_n(T)/dT$. Since $s_n(T)$ and $e_n(T)$ contain both, $c_n(T)$ and $c_n'(T)$, they serve for a more sensitive test of the model than considering $c_n(T)$ alone. Estimating $c_n'(T)$ through a fine but finite difference approximation of $c_n(T)$, we compare QPM with lattice QCD results [24] for $s_{2,4}$ and $e_{2,4}$ in Fig. 2 and find a fairly good agreement. The pronounced structures in the vicinity of the transition temperature follow from the change in the curvature of $G^2(T, \mu_q = 0)$ at $T = T_c$.

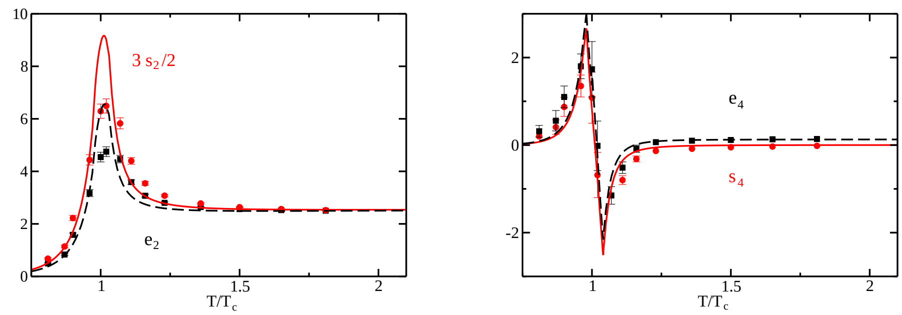

Fig. 2. Comparison of our QPM with lattice QCD results [24] for $e_n(T)$ (squares) and $s_n(T)$ (circles) as function of T/T_c for $N_f = 2$; left (right) panel for $n = 2\,(4)$. QPM parameters: $\lambda = 12$, $T_s = 0.87T_c$, $b = 426.1$ with $T_c = 175$ MeV as adjusted to $c_2(T)$ from [26] (cf. [22]). We choose $\Delta T = 5.25$ MeV for suitably estimating $c_n'(T)$ by finite difference approximation of $c_n(T)$.

Assuming local entropy and baryon number conservation during the hydrodynamical expansion of the fireball created in heavy-ion collisions, the strongly interacting system evolves isentropically. The evolutionary paths of individual fluid elements can be displayed by trajectories $s/n_B = const$ in the T - μ_B plane. We calculate n_B and s from (5) up to $\mathcal{O}((\mu_B/T)^6)$ for the isentropic trajectories $s/n_B =$ 300, 45 and compare with lattice QCD results [24] in Fig. 3. Finding a fairly good agreement, the pattern of the evolutionary paths is mainly influenced by $s_0(T)$. For instance, in the vicinity of T_c a larger value of $s_0(T)$ of about 30% translates into a 28% increase in μ_B for the same trajectory. At large T, where $c_{0,2}(T)$ are essentially

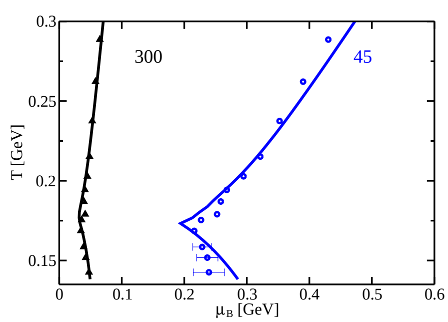

Fig. 3. Isentropic trajectories: Comparison of $N_f = 2$ lattice QCD results [24] for $s/n_B = 300$ (triangles) and 45 (circles) with the corresponding QPM results. The physical scale is $T_c = 175$ MeV.

flat, the relation $\frac{\mu_B}{T} = 18\frac{c_0}{c_2}(\frac{s}{n_B})^{-1}$ holds for small μ_B, i. e. lines of constant specific entropy are given by lines of constant μ_B/T.

Along the isentropic trajectories, we evaluate the EoS $p(e)$. As depicted in Fig. 4 (left panel), the EoS, reproducing the lattice QCD results impressively well, is found to be almost independent of the considered specific entropy. Accordingly, the speed of sound $v_s^2 = \partial p/\partial e$ as exhibited in the right panel of Fig. 4 is also rather independent of s/n_B.

4. Conclusions

We presented a comparison of our QPM with recent two-flavour lattice QCD results of the isentropic equation of state at finite baryo-chemical potential. In particular, we focused on the Taylor expansion coefficients of energy density and entropy density, reproducing the pronounced structures in the vicinity of the (pseudo-) critical temperature fairly well. In addition, the isentropic trajectories in the T - μ_B plane were compared. The EoS along those paths of constant entropy per baryon was found to be rather independent of the particular value of specific entropy. Having tested the successful applicability of our model in the finite μ_B - region for $N_f = 2$, one can proceed to the physically interesting case of $N_f = 2 + 1$ quark flavours and extend the EoS $p(T)$ towards finite baryon densities. Such an EoS can be applied to the hydrodynamical stage of heavy-ion collisions, e. g. by studying transverse momentum spectra and differential elliptic flow of various hadron species. This will be reported elsewhere.

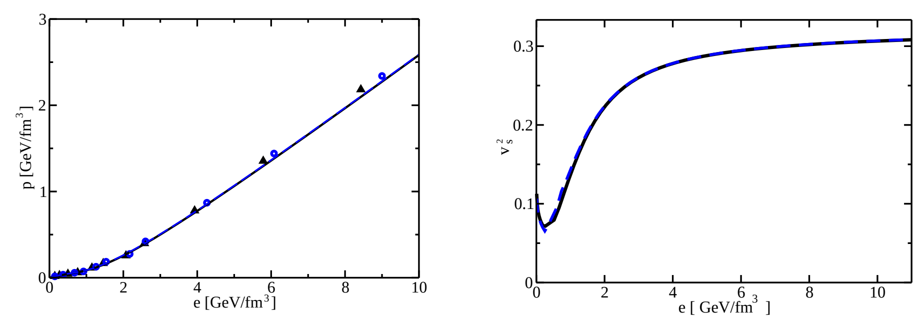

Fig. 4. Left panel: comparison of lattice QCD results [24] of p as function of e for $N_f = 2$ along $s/n_B = 300$ (triangles) and 45 (circles) with corresponding QPM results depicted by solid and dashed lines, respectively. Right panel: according speed of sound v_s^2.

Acknowledgment(s)

This work is supported by BMBF 06 DR 121, GSI and Helmholtz association VI. We thank F. Karsch, E. Laermann, A. Peshier and K. Redlich for fruitful discussions.

References

1. P. F. Kolb and U. Heinz, *Quark Gluon Plasma 3*, eds R.C. Hwa and X.N. Wang, World Scientific, Singapore, p. 634
2. P.F. Kolb, P. Huovinen, U. Heinz and H. Heiselberg, Phys. Lett. **B500** (2001) 232
3. D. Teaney, J. Lauret and E.V. Shuryak, Phys. Rev. Lett. **86** (2001) 4783
4. E.V. Shuryak, Prog. Part. Nucl. Phys. **53** (2004) 273
5. U. Heinz, J. Phys. **G31** (2005) 717
6. P. Huovinen, Nucl. Phys. **A761** (2005) 296
7. P. Huovinen and P.V. Ruuskanen, preprint nucl-th/0605008
8. P. Levai and U. Heinz, Phys. Rev. **C57** (1998) 1879
9. D.H. Rischke, Prog. Part. Nucl. Phys. **52** (2004) 197
10. R.A. Schneider and W. Weise, Phys. Rev. **C64** (2001) 055210
11. J. Letessier and J. Rafelski, Phys. Rev. **C67** (2003) 031902
12. A. Rebhan and P. Romatschke, Phys. Rev. **D68** (2003) 025022
13. M.A. Thaler, R.A. Schneider and W. Weise, Phys. Rev. **C69** (2004) 035210
14. Yu.B. Ivanov, V.V. Skokov and V.D. Toneev, Phys. Rev. **D71** (2005) 014005
15. A.S. Khvorostukin, V.V. Skokov, V.D. Toneev and K. Redlich, preprint nucl-th/0605069
16. V.N. Bannur, preprint hep-ph/0508069; hep-ph/0602222; hep-ph/0604158
17. A. Peshier, B. Kämpfer, O.P. Pavlenko and G. Soff, Phys. Lett. **B337** (1994) 235; Phys. Rev. **D54** (1996) 2399; A. Peshier, B. Kämpfer and G. Soff, Phys. Rev. **C61** (2000) 045203; Phys. Rev. **D66** (2002) 094003
18. R.D. Pisarski, Nucl. Phys. **A498** (1989) 423c
19. M. Le Bellac, *Thermal Field Theory*, Cambridge University Press, Cambridge, 1996
20. M.I. Gorenstein and S.N. Yang, Phys. Rev. **D52** (1995) 5206
21. M. Bluhm, B. Kämpfer and G. Soff, J. Phys. **G31** (2005) 1151
22. M. Bluhm, B. Kämpfer and G. Soff, Phys. Lett. **B620** (2005) 131
23. M. Bluhm, Diploma Thesis, Technische Universität Dresden, August 2004
24. S. Ejiri, F. Karsch, E. Laermann and C. Schmidt, Phys. Rev. **D73** (2006) 054506
25. F. Karsch, E. Laermann and A. Peikert, Phys. Lett. **B478** (2000) 447
26. C.R. Allton, S. Ejiri, S.J. Hands, O. Kaczmarek, F. Karsch, E. Laermann and C. Schmidt, Phys. Rev. **D68** (2003) 014507; C.R. Allton, M. Doring, S. Ejiri, S. J. Hands, O. Kaczmarek, F. Karsch, E. Laermann and K. Redlich, Phys. Rev. **D71** (2005) 054508
27. F. Karsch, Nucl. Phys. Proc. Suppl. **83** (2000) 14